Molecular Crystals and Liquid Crystals
Publication details, including instructions for authors and subscription information:
http://www.tandfonline.com/loi/gmcl16

# Electro-Optical Behavior of a Novel Strong-Weak and Weak-Weak Anchored Large-Pitch Cholesteric

H. P. Hinov [a], E. Kukleva [a] & A. I. Derzhanski [a]
[a] Institute of Solid State Physics, Boul. Lenin 72, Sofia, 1184, Bulgaria
Version of record first published: 17 Oct 2011.

To cite this article: H. P. Hinov , E. Kukleva & A. I. Derzhanski (1983): Electro-Optical Behavior of a Novel Strong-Weak and Weak-Weak Anchored Large-Pitch Cholesteric, Molecular Crystals and Liquid Crystals, 98:1, 109-124

To link to this article: http://dx.doi.org/10.1080/00268948308073466

*Mol. Cryst. Liq. Cryst.*, 1983, Vol. 98, pp. 109–124
0026-8941/83/9804–0109/$18.50/0




# Electro-Optical Behavior of a Novel Strong-Weak and Weak-Weak Anchored Large-Pitch Cholesteric†

H. P. HINOV, E. KUKLEVA and A. I. DERZHANSKI

*Institute of Solid State Physics, Boul. Lenin 72, Sofia 1184, Bulgaria*

*(Received January 31, 1983)*

The electro-optical behavior of strong-strong, strong-weak and weak-weak anchored tilted and reversely-tilted large-pitch cholesterics has been investigated. The weak anchoring has been achieved after rubbing with soap the previously mechanically-rubbed glass plates. Under a voltage excitation, the most important reversely-tilted weak-weak anchored cholesteric layers giving rise to a nearly-planar Grandjean-like texture showed the appearance of a Helfrich's instability, followed by a $\pi/2$ rotation of the helix and finally, a scroll texture which compactly disappeared into a completely unwinded cholesteric. When voltage was switched off, the unwinded cholesteric was returned to the initial Grandjean-like texture for the case of a low voltage ($U < 3U_{th}$, where $U_{th}$ is the threshold voltage for the Helfrich's instability) or has been transformed into a finger-print texture for higher voltages. This novel boundary-induced bi-stability is related to the weakness of the surface anchoring.

In addition, attention has been paid on the important electro-optical behavior of the well-known, however insufficiently investigated, finger-print texture embedded into a homeotropic matrix.

## I. INTRODUCTION

The electro-optical phenomena in cholesteric liquid crystals (ChLCs) with a large pitch $p$ comparable to or larger than the thickness $d$ of the cholesteric layer ($p \gtrsim d$) have been intensively studied in the last ten years due to the successful application of the electrically-induced cholesteric-nematic (Ch–N) phase change in the indicator technique.[1–6]

† This paper was presented at Ninth International Liquid Crystal Conference, Bangalore, India, December 6–10, 1982.

The experimental investigations of the electrically-induced or magnetically-induced Ch–N phase change accompanied by creation of various textures including the finger-print (more generally confocal) texture, the scroll texture (or more correctly disclination patterns), the Grandjean's texture and the homeotropic orientation due to the complete unwinding of the cholesteric helix[7–18] as well as the theoretical effort[10,16,19–30] shed a considerable light on many questions related to this effect. In addition, these investigations showed the complexity of the dynamics of this effect leading to one-stable, bi-stable, tri-stable and persistent electro-optical behavior of the liquid crystal (LC) and to a strong hysteresis.[27,31–34] On the other hand, the experimental and theoretical investigations of the cholesteric-nematic phase change are often complicated by the presence of a number of various disclinations, walls and even dislocations in the cholesteric planes.[35–41]

It is evident that the unwinding of the cholesteric helix with a large pitch that is comparable to the thickness of the cholesteric layer, depends not only on the action of external forces (electric or magnetic fields, etc.) but also on the surface treatment and the strength of the surface anchoring of the cholesteric molecules. The influence of the surface anchoring of the cholesteric layer is so important that it can determine the equilibrium pitch of the Ch. For instance, our experimental investigations unambiguously pointed out that the pitch of the strongly-anchored Ch is considerably smaller relative to the pitch of the same Ch in the case of weak anchoring. This is true not only for the planar Grandjean-like texture but also for the con-focal textures; i.e. the natural cholesteric pitch is undisturbed for the large-pitch Chs only in the case of weak anchoring of the LC molecules. Unfortunately, this important question has been insufficiently investigated up to now.[42–50] According to Lin-Hendel's results[24,34] the occurrence of the observed tri-stability is a result of the balance between the surface anchoring and the cholesteric nature of the material. In general, the surface forces act strongly on large-pitch Chs and weakly on short-pitch Chs. For example, according to Price and Bak's results,[48] the surface forces can orient the short-pitch Chs with a pitch in the range of several microns only along a distance of 50 microns; i.e. the penetration depth of the surface forces in this case is comparable to that of the corresponding smectic surface forces and is much smaller than the penetration depth of the surface forces into N layers.[51,52]

The aim of this paper is only to give a qualitative description of the electro-optical behavior of the Ch–N phase change for Chs with a large pitch (in our case the thickness-to-pitch ratio was smaller than 0.2) strong-weak or weak-weak anchored by the appropriate treatment of the glass plates confining the LC (we used a.c. electric field at 5 kHz to avoid the

creation of electrohydrodynamic effects). The small thickness-to-pitch ratio usually determines a nematic rather than a cholesteric phase.[12,13,24,34] However, this is true only for a strong surface anchoring of the cholesteric layer. The weak surface anchoring usually determines a well-defined finger-print texture. For instance, our results obtained with large-pitch Chs ($d/p < 0.2$) as well as the results obtained by Hirata *et al.*[23] who are able to obtain a stripe domain with a periodicity of 250 microns confirm this claim.

Our experimental results revealed the crucial role of the weak anchoring for the creation of a nearly planar Grandjean-like texture in the special case of reversely-tilted layers. Under a.c. voltage excitation, the planar (or nearly planar) cholesteric layers are undulated; i.e. one appears as the Helfrich's instability, followed by a $\pi/2$ rotation of the helix, or the creation of a finger-print texture, which at a higher voltage disappeared and a pseudo-nematic is formed. Inversely, at the switch off of the voltage, the unwinded cholesteric can relax into the initial planar Grandjean-like texture or can be transformed into a finger-print texture depending on the value of the surface tilt resp. on the voltage strength. In this way, we observed *a novel bi-stable boundary-induced effect* which might be useful for industrial applications. On the other hand, a special attention was paid to the important electro-optical behavior of the already known, however insufficiently investigated, finger-print texture embedded into a homeotropic matrix.

## II. LIQUID CRYSTAL CELLS

From our recent investigations it is known that the soap treatment of the glass plates is able to determine a weak nondegenerated $\theta$-polar surface anchoring of the MBBA LC.[52–58] A more effective utilization of this surfactant was obtained by rubbing of previously rubbed glass plates. In this way, according to the Nakamura's results,[59] it is possible to *pre-determine* the sign of the tilt angle at the boundaries. This result was confirmed in our recent investigations. Moreover, the LC bias surface angle depends strongly on the soap thickness (this problem has not been resolved in detail) as follows: the thick soap deposition always leads to a large bias angle which is in the range of 10–20° relative to the glass plate normal; whereas, the thin soap deposition determines a small surface tilt being in the range of 50–60°. Under a thick soap deposition we mean such a deposition which is observable with a naked eye and under a thin soap deposition, the nonobservable soap layer. It seems that the soap either completely covers the glass plate topography or the deeper grooves and at the same time remembers the

rubbing direction; i.e. the first soap layers which are sensitive to this direction probably act on the whole soap layer. In this way, the rubbing of the glass plates determines an oriented soap layer. This important problem can be resolved either by attenuated total internal reflection measurements[60] or by NMR measurements.[61] In addition, the soap deposition may considerably reduce the surface inhomogeneities able to prevent the long-time stability of the unwinded cholesteric state since the slow return from the pseudonematic to the focal-conic texture always starts at surface defects.

The long-pitch cholesteric was produced by doping a small percentage (1% wt.) of a cholesteril chloride (CC) into a mixture of a nematic host consisting of 89% wt. MBBA and 10% wt. 5CB with a high positive dielectric anisotropy.[62] The percentage of 5CB was chosen to ensure a small positive dielectric anisotropy of the mixture. Using the dielectric anisotropy measurements performed by Park and Labes on a MBBA-5CB mixture[63] and having in mind the value of the dielectric anisotropy of the CC, which although positive is small ($\Delta\varepsilon \sim +3$[17]), we evaluated the dielectric anisotropy of the Ch-N mixture under study to be in the range between 1.5 and 2. The percentage of the CC was chosen to ensure the formation of a large-pitch cholesteric with a thickness-to-pitch ratio below 0.25.

All untreated glass plates were initially rubbed with a diamond paste (a grain size around 0.5 $\mu$m). Occasionally we used glass plates covered with a thin SiO film deposited under vacuum evaporation. Strong-weak anchoring was achieved after the repeatable rubbing of one of the glass plates confining the LC under study with soap. Weak-weak anchoring was achieved by rubbing of both glass plates with soap. In addition, the upper glass plate had two positions determining in this way either a uniform tilt or a reversely tilted deformation in the cells under study. The second position was obtained after a $\pi/2$ rotation of the glass plate. All the possible LC orientations in such cells are summarized in Figure 1 and include a tilted or reversely tilted LC orientation for the case of nontreated with soap rubbed glass plates and a tilted or reversely tilted LC orientation for the case of soap-treated glass plates. As mentioned, the latter case can be divided into a strong-weak anchored reversely tilted LC orientation when one of the glass plates is soap-treated and a weak-weak anchored reversely tilted LC orientation when both glass plates are soap-treated. Let us note that the optical observations on a number of MBBA-5CB mixtures performed under a polarizing microscope unambiguously show that the rubbing itself is not able to produce planar alignment of the LC mixture. This experimental finding is due to the much smaller LC planar alignment capability of the rubbing method relative to the ruled-gratings[64] or the well-known Janning's method,[65] as well as to the tendency for a homeo-

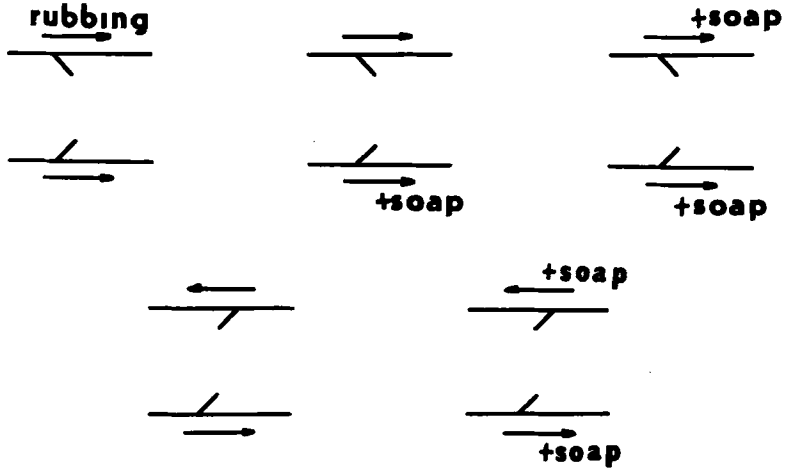


FIGURE 1 A schematic representation of the surface orientation of a large-pitch cholesteric-nematic mixture for all considered in the text cases.

tropic orientation of the LC 5CB on treated or nontreated glass plates.[66–68] On the other hand, the experimental results also depend on the nature of the conductive coating of the glass plates.[69]

## III. EXPERIMENTAL RESULTS AND CONSIDERATIONS

Let us start with the most interesting and important case:

### IIIA. Strong-strong, strong-weak and weak-weak reversely tilted MBBA-5CB-CC layers

*(1) Strong-strong reversely tilted MBBA-5CB-CC layers* Reversely tilted cholesteric layers with a large pitch (the thickness-to-pitch ratio was below 0.25) obtained with usual rubbed glass plates showed a fingerprint texture embedded into a homeotropic matrix[70] (see Figure 2). Although this texture is well known,[19,20,22] no attention has been paid on its remarkable electro-optical properties. See the electro-optical curves and the discussion given below. This structure appears to be very stable and reproducible in reversely tilted cholesteric layers when the reverse tilt at the boundaries is achieved by rubbing. This kind of structure, usually existing in homeotropic or nearly homeotropic films, unambiguously pointed out that the tilting of the LC molecules at the surfaces is above 45° and that the anchor-

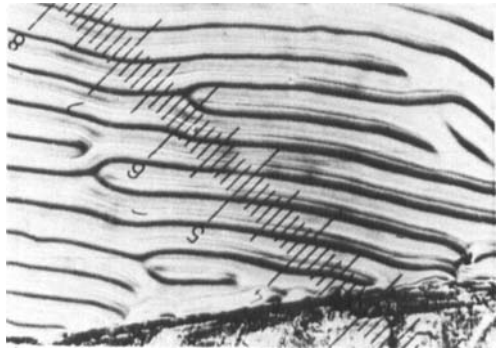

FIGURE 2 A finger-print texture embedded into a homeotropic matrix; a reversely-tilted orientation of a MBBA-5CB-CC mixture 15 microns thick at room temperature; crossed nicols, 10 divisions correspond to 45 microns.

ing is not so strong. Under the combined action of the reverse tilt at the two boundaries and the intrinsic twist force due to the cholesteric nature of the MBBA-5CB-CC mixture, a well-defined fingerprint texture embedded into a homeotropic matrix is formed. However, the eventual inclination of the molecules in the surface regions is not known and this problem can be successfully resolved, for instance, with the aid of the total internal reflection of a laser beam.

*(2) Reversely tilted strong-weak anchored MBBA-5CB-CC layers* The strong-weak anchored reversely tilted cholesteric layers display a very large variety of textures depending on the soap thickness which was not controllable in our experiment. For example, we obtained either many Grandjean-like regions separated by walls and disclinations (see Figure 3) (let us note that the Grandjean-like orientation was near the soap-treated glass plate as proved by the microscopic observations), or the so-called scroll texture which usually has no spirales and contains many disclinations[17] and dislocations (Figure 4) and finally, the most typical and important novel texture shown in Figure 5 which consists of large-area regions with a Grandjean-like orientation separated by different disclinations and walls. The stripes, visible on the picture, depend on the position of the nicols and probably represent the total optical effect due to the slight inclination of the cholesteric axis relative to the glass plate normal. This assumption was confirmed by the voltage excitation of a number of reversely tilted weak-weak anchored cholesteric layers leading to the development of a regular Helfrich's instability.

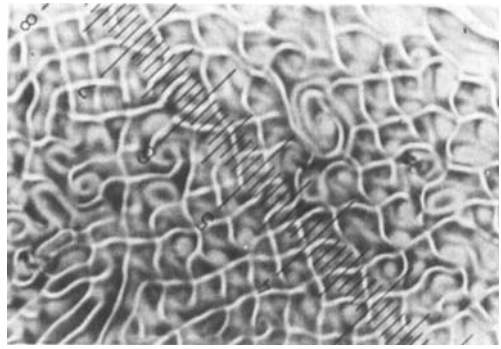

FIGURE 3 Many small Grandjean-like regions separated by walls and disclinations in a reversely-tilted strong-weak anchored MBBA-5CB-CC mixture 15 microns thick at room temperature; crossed nicols, 10 divisions correspond to 45 microns.

*(3) Reversely tilted weak-weak anchored MBBA-5CB-CC layers* In the most important and interesting case of reversely tilted weak-weak anchored cholesteric layers we observed a homogeneous Grandjean-like texture which was in some cases with a slight inclination of the cholesteric axis (Figure 6). The polarizer rotation at an angle of about 40° led to more distinct and visible stripes (Figure 7).

## IV. ELECTRO-OPTICAL BEHAVIOR

The electric field-induced textures and the phase-change behavior of the long-pitch cholesteric films are summarized in Table I. For convenience, the corresponding electric field-induced textures, obtained by Lin-Hendel in planar and homeotropic cholesterics[24,34] are given as well. In spite of the Lin-Hendel's results, the bi-stability behavior observed in our experiment depends crucially on the boundary conditions. At this stage of the experimental investigations, however, we do not know exactly the role of the thickness-to-pitch ratio. It is only evident that the boundary conditions are not so important for large ratios. Furthermore, the small thickness-to-pitch ratio usually leads to the creation of a fingerprint texture. Let us stress that the focal-conics are usually not sensitive to the nicol position and to the polarization of the light whereas this is not true for one well-aligned fingerprint texture. Let us discuss these cases in more detail. To our knowledge, the possible transformations of the fingerprint texture embedded into a homeotropic matrix under a voltage excitation have not been studied in

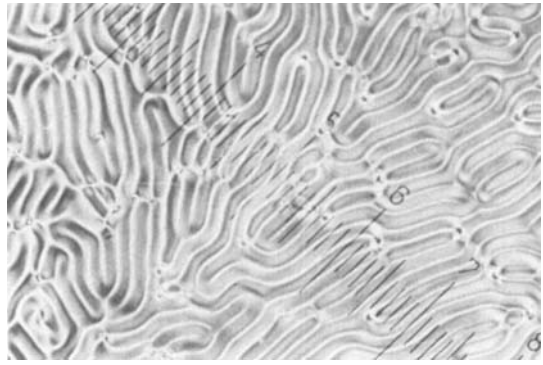

FIGURE 4 A scroll texture in a MBBA-5CB-CC mixture 15 microns thick at room temperature; crossed nicols, 10 divisions correspond to 45 microns.

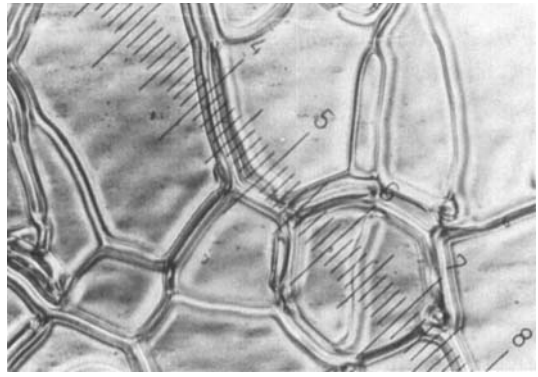

FIGURE 5 Large Grandjean-like regions separated by walls and disclinations in a reversely-tilted strong-weak anchored MBBA-5CB-CC mixture 15 microns thick at room temperature; the stripes show the inclination of the cholesteric axis relative to the glass plate normal; crossed nicols, 10 divisions correspond to 45 microns.

detail up to now. Our qualitative results unambiguously show that this structure exhibits the smallest threshold voltage which was below 1 V. Let us recall that the dielectric anisotropy of the cholesteric-nematic mixture under study is between 1.5 and 2. Consequently, in the case of a large positive dielectric anisotropy, the voltage threshold should be in the MILLIVOLT region. This is the fastest mode observed among the other cholesteric textures investigated in our experiment. Further, after an abrupt switch off of the voltage the LC returns to its equilibrium state (Figure 8); i.e. this structure does not display a bi-stable behavior. Our visual observations,

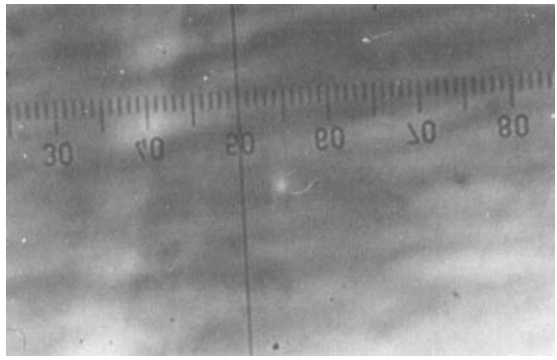

FIGURE 6 A Grandjean-like texture with a slight inclination of the cholesteric axis relative to the glass plate normal in a reversely-tilted weak-weak anchored MBBA-5CB-CC mixture 15 microns thick at room temperature; crossed nicols, 10 divisions correspond to 54 microns.

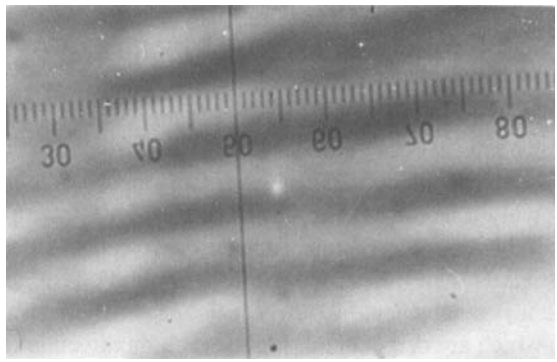

FIGURE 7 The same picture; the polarizer was rotated at about 40°.

however, clearly show the existence of a hysteresis which depends on the competition between the relaxation time of the surface deformation and the voltage change rate. The existence or nonexistence of an eventual hysteresis in all cases under consideration will be published separately.

Under a voltage excitation, the reversely tilted strong-weak cholesteric layer is transformed into a focal-conic texture and finally, into a homeotropic unwinded cholesteric. The abrupt switch off of the voltage led again to the creation of the focal-conic texture (Figure 8). Consequently, this structure shows a bi-stable electro-optical behavior. However, this type of surface anchoring is not convenient for display applications due to the large variety of the textures observed, to the slow relaxation and the high voltage

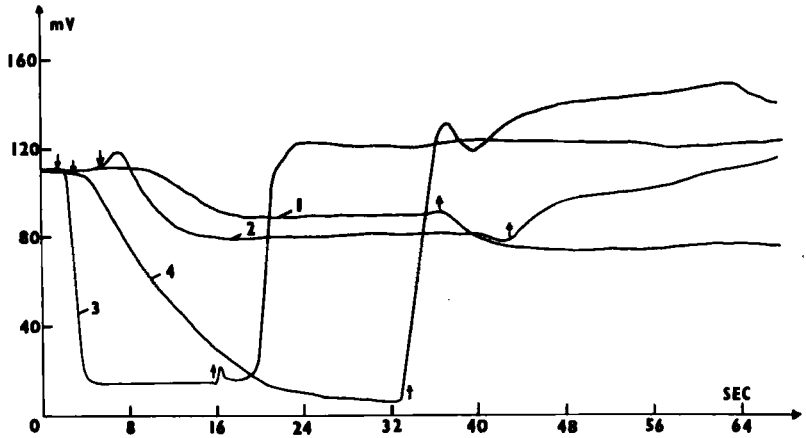


FIGURE 8 Electro-optical transmission curves for a reversely-tilted strong-weak (curve 1, U = 10 V, $U_{th}$ = 5 V), weak-weak (curve 2, U = 4 V, $U_{th}$ = 2 V), weak-weak (curve 4, U = 15 V, $U_{th}$ = 2 V) anchored MBBA-5CB-CC mixture 15 microns thick at room temperature. The curve 3 corresponds to the case of a finger-print texture embedded into a homeotropic matrix at the same conditions, U = 4 V, $U_{th}$ = 2 V.

which is needed. For instance, the voltage necessary to unwind completely the cholesteric was in the range of 15–20 V.

The electro-optical behavior of the most interesting and important weak-anchored reversely tilted cholesteric layers shows the following sequence of events (see Table I); at increasing of the voltage the stripes become more clear. One observes the further inclination of the cholesteric axis relative to the glass plate normal (Figure 9). An appearance of Helfrich's instability shows stripes which are perpendicular to the rubbing direction (Figure 10). In Lin-Hendel's results this instability corresponds to cross-hatched patterns. Development of this instability (Figure 11), its transformation into a fingerprint texture obtained by a $\pi/2$ rotation of the helix axis (Figure 12) and a transformation of the fingerprint texture into a scroll texture which is very near to the glass plate finally is compactly transformed into a completely unwinded homeotropic cholesteric state. Let us note that the fingerprint texture usually is transformed into a cholesteric unwinded homeotropic state by annihilation of the available disclinations and by obtaining of a number of fingers embedded into a homeotropic matrix which finally disappeared after a fast collapsing. The electro-optical behavior of these cells depends on the strength of the voltage applied across the cholesteric layer under study. For example, when the value of the voltage was approximately between $U_{th}$ ($U_{th}$ is the threshold voltage) and $3U_{th}$ the cholesteric LC had been fastly returned in its initial position after the switch

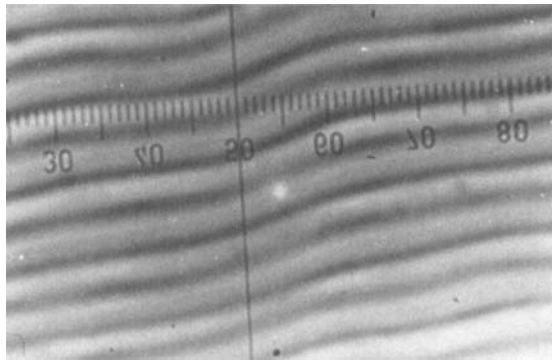

FIGURE 9 Voltage-induced stripes in a Grandjean-like texture in a reversely-tilted weak-weak anchored MBBA-5CB-CC mixture 15 microns thick at room temperature, U = 2 V, f = 1 kHz, crossed nicols, 10 divisions correspond to 54 microns.

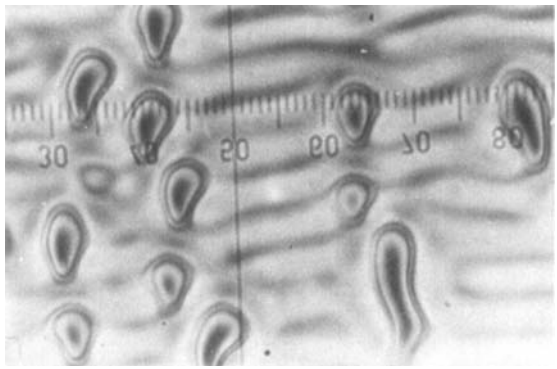

FIGURE 10 The same LC layer; appearing of the Helfrich's instability, U = 2 V, f = 1 kHz.

off of the voltage (Figure 8). However, when the excitating voltage was above $3U_{th}$, the homeotropic pseudonematic had been transformed into a well-defined fingerprint texture after the switch off of the voltage. The corresponding electro-optical transmission curve clearly shows a bi-stable electro-optical behavior of such a cell. We relate this electro-optical bi-stability to the *weakness* of the surface anchoring which dictates a nearly planar position of the cholesteric planes (a Grandjean-like texture) in the voltageless state. Whereas, the application of a high ac voltage which was above 10 V, led to homeotropic orientation of the cholesteric layer not only in the bulk but also in the boundary regions. It led to a complete homeo-

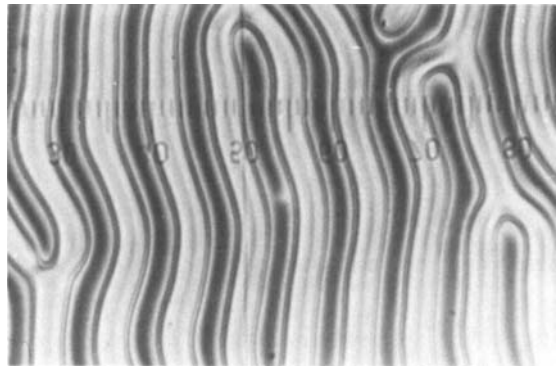

FIGURE 11 The same LC layer; development of the Helfrich's instability, U = 2,1 V, f = 1 kHz.

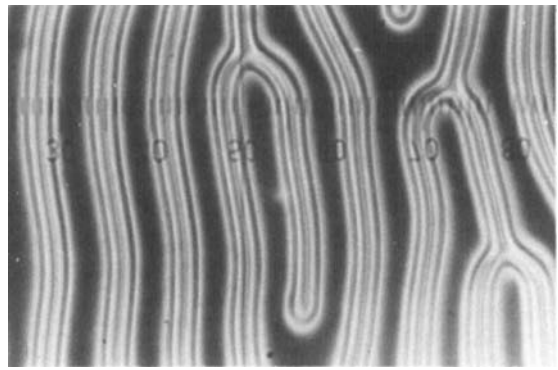

FIGURE 12 The same LC layer; a $\pi/2$ rotation of the cholesteric axis: appearance of a finger-print texture, U = 2,7 V, f = 1 kHz.

tropic orientation of the LC due to the total unwinding of the cholesteric. On the other hand, it is well-known that the fingerprint textures are usually formed in cases when the orientation of the molecules at the boundaries is homeotropic[19,20] and because of that the completely unwinded cholesteric relaxed into a well-defined fingerprint texture. It is clear that this surface-induced bi-stability depends strongly on the ratio between the rate of the voltage decrease and the relaxation of the surface deformation, on the eventual presence of disclinations or their associations, etc. These disclinations can increase the elastic energy of the fingerprint texture and can transform the cholesteric state into a metastable state with energy which is higher relative to that of the Grandjean-like texture. All these problems

await their further elaboration. It is necessary to point out that our results nearly coincide with those obtained by Lin-Hendel for the Ch-N phase change of planar layers[24,34] (see Table I). However, the final relaxation texture in the Lin-Hendel's observations has usually been the con-focal texture which can be nucleated on glass plate irregularities and which is not dependent on the surface LC orientation.

### IVA. Tilted strong-strong and weak-weak anchored MBBA-5CB-CC layers

The cholesteric textures observed as well as the electro-optical transmission curves obtained shown in Figure 13 clearly pointed out the similarity between these two cases. These were expressed by the creation of a fingerprint texture which entirely covers the LC area before the voltage application and which returns to a fingerprint texture embedded into a homeotropic matrix after the switch off of the voltage. In these cases we observed a weak bi-stability. The difference in the electro-optical behavior is due to the very cholesteric pictures which are inherent for these two cases. In usual tilted LC layers, the fingers were nearly randomly oriented relative to the rubbing axis and the total electro-optical response was weak (Figure 13). In tilted

TABLE I

Texture and phase changes of LC films as a function of applied voltages and surface anchoring

| Boundary conditions | V = 0 | $\uparrow V > 3U_{th}$ $\uparrow V = V_f^{24}$ | $V_{quenched}$ | $\uparrow V > U_{sat}$ | $V_{quenched}$ |
|---|---|---|---|---|---|
| Reversely-tilted strong-strong anchored Ch layers | $FPT_N$ | | $FPT_N$ | NT | $FPT_N$ |
| Reversely-tilted strong-weak anchored Ch layers | TG + disclin. | | FCT | NT | FCT |
| Reversely-tilted weak-weak anchored Ch layers | TG | Helfrich's instability | TG | NT | FPT $TG(V < 3U_{th})$ |
| Tilted strong-strong anchored Ch layers | Nonoriented FPT | | Nonoriented $FPT_N$ | NT | Nonoriented $FPT_N$ |
| Tilted weak-weak anchored Ch layers | Oriented FPT | | Oriented $FPT_N$ | NT | Oriented $FPT_N$ |
| Homeotropic: Lin-Hendel[24] | ST/G | FCT | FCT | NT | ST |
| Homogeneous: Lin-Hendel[24] | G | FCT | FCT | NT | FCT |

FPT — fingerprint texture; G — Grandjean's plane texture; NT — no texture; TG — tilted Grandjean's plane texture; $FPT_N$ — fingerprint texture embedded in a homeotropic matrix; FCT — focal-conic texture; ST — scroll texture

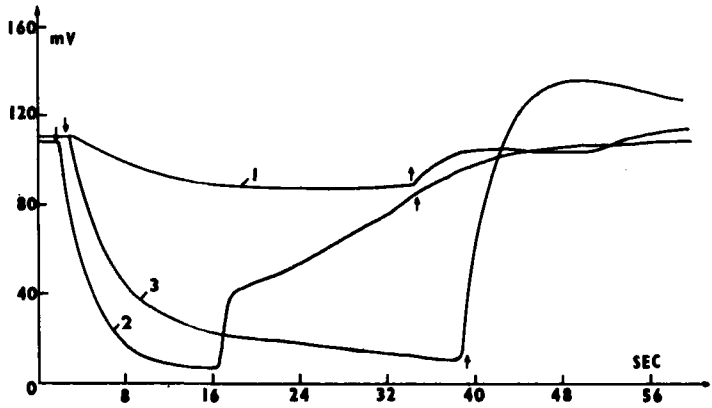


FIGURE 13 Electro-optical transmission curves for a tilted strong-strong (curve 1, $U = 5$ V, $U_{th} = 1{,}5$ V) and weak-weak (curve 2, $U = 5$ V, $U_{th} = 2$ V, $A \perp P \| n_0$, curve 3, $U = 5$ V, $U_{th} = 2$ V, $A \perp P$ 45° $n_0$) anchored MBBA-5CB-CC mixture 15 microns thick at room temperature.

weak-weak anchored layers, however, the fingers were completely oriented along the rubbing direction and the corresponding electro-optical transmission curves depended strongly on the nicol position (Figure 13). Furthermore, the soap treatment of the glass plates was accompanied by a considerable decrease in the number of the various disclinations and dislocations.

## V. CONCLUSIONS

The electro-optical behavior of large-pitch cholesterics with positive dielectric anisotropy and a thickness-to-pitch ratio below 0.25 strongly depends on the electrode treatment and surface anchoring. In spite of Lin-Hendel's results,[24,34] the observation of the electric field-induced textures and phase transformations in tilted and reversely tilted strong-weak and weak-weak anchored cholesteric layers achieved by rubbing of the glass plates followed by soap deposition on one of them (strong-weak anchoring) or on the both (weak-weak anchoring) as well as the electro-optical characteristic curves unambiguously pointed out the existence of surface-induced electro-optical bi-stability due to the weak anchoring which might be important for the large-area LC indicators and screens.

The creation of a nearly-homogeneous Grandjean-like texture in reversely tilted layers when the glass plates are soap-treated is a result which is not achievable in usual reversely tilted cholesteric layers when the glass plates

are only rubbed. The usual technique for obtaining of a Grandjean-like texture with large-pitch cholesterics by SiO treatment of the glass plates under vacuum evaporation can be successfully replaced by the more simple rubbing and soap-deposition technique.

The phenomena observed are characteristic only for the long-pitch cholesterics when the pitch is comparable to and larger than the thickness of the cholesteric layer. Any increase in the value of the thickness-to-pitch ratio will remove these results.

In addition, we show the importance of the well-known, however insufficiently investigated up to now, fingerprint texture embedded into a homeotropic matrix and give a promising method for its creation. Our experimental results clearly show that the operating voltage of such a structure can decrease below 1 V for a sufficiently high dielectric anisotropy. In our opinion, this texture can ensure the smallest threshold voltage and fastest response times among all known cholesteric textures.

A number of important problems such as the hysteresis and the more detailed quantitative description of the Helfrich's instability will be discussed in other papers.

## References


1. W. J. S. Blackburn, *J. Phys. D: Appl. Phys.*, **13**, 1785 (1980).
2. M. Schadt and P. Gerber, *Mol. Cryst. Liq. Cryst.*, **65**, 241 (1981).
3. P. Gerber, *Z. Nat.*, **36a**, 718 (1981).
4. Jing-an Zhao, Tong-Shon-Sheng and Ruan Liang, *Wuli (China)*, **2**, 10 (1980).
5. J. A. I. Mazur and A. A. Doroshkin, *Electron. Prom.*, **7**, 49 (1978).
6. Y. Nara and Sh. Kobayashi, *J. Appl. Phys.*, **49**, 4277 (1978).
7. F. Rondelez and H. Arnould, C. R. Acad. Sc Paris, *t. 273*, B549 (1971).
8. I. Rault and P. Cladis, *Mol. Cryst. Liq. Cryst.*, **15**, 1 (1977).
9. H. Kelker, *Mol. Cryst. Liq. Cryst.*, **15**, 347 (1972).
10. P. E. Cladis and M. Kléman, *Mol. Cryst. Liq. Cryst.*, **16**, 1 (1972).
11. J. Rault, *Liq. Cryst. Ord. Fl.*, **2**, 677 (1974).
12. F. Rondelez, Ph. Dr. Thesis, Orsay, France (1973).
13. F. Rondelez and J. P. Hulin, *Sol. St. Comm.*, **10**, 1009 (1972).
14. T. J. Scheffer, *Phys. Rev. Lett.*, **28**, 593 (1972).
15. J. P. Hulin, *Appl. Phys. Lett.*, **21**, 455 (1972).
16. H. Hervet, J. P. Hurault and F. Rondelez, *Phys. Rev.*, **A8**, 3055 (1973).
17. W. Greubel, U. Wolff and H. Krüger, *Mol. Cryst. Liq. Cryst.*, **24**, 103 (1973).
18. K. H. Walter and H. H. Krüger, *Ber. Bunsges. Phys. Chem.*, **Bd 78**, 912 (1974).
19. M. J. Press and A. S. Arrott, *J. Physique*, **37**, 387 (1976).
20. M. J. Press and A. S. Arrott, *Mol. Cryst. Liq. Cryst.*, **37**, 81 (1976).
21. T. Akahane, M. Nakao and T. Tako, *Jpn. J. Appl. Phys.*, **16**, 241 (1977).
22. A. E. Stieb, *J. Physique*, **41**, 961 (1980).
23. Sh. Hirata, T. Akahane and T. Tako, *Mol. Cryst. Liq. Cryst.*, **75**, 47 (1981).
24. C. G. Lin-Hendel, *J. Appl. Phys.*, **53**, 916 (1982).
25. P. G. de Gennes, *Sol. St. Comm.*, **6**, 163 (1968).
26. R. B. Meyer, *Appl. Phys. Lett.*, **12**, 281 (1968).
27. W. Helfrich, *Appl. Phys. Lett.*, **17**, 531 (1970).

28. J. P. Hurault, *J. Chem. Phys.*, **59**, 2068 (1973).
29. J. M. Delrieu, *J. Chem. Phys.*, **60**, 1081 (1974).
30. G. Vertogen and E. W. C. van Groesen, *J. Chem. Phys.*, **76**, 2043 (1982).
31. M. Kawachi and O. Kogure, *Jpn. J. Appl. Phys.*, **16**, 1673 (1977).
32. S. K. Kwok and Y. Liao, *J. Appl. Phys.*, **49**, 3970 (1978).
33. M. Kawachi, O. Kogure and K. Kato, *Jpn. J. Appl. Phys.*, **17**, 391 (1978).
34. C. G. Lin-Hendel, *Appl. Phys. Lett.*, **38**, 615 (1981).
35. Y. Bouligand and M. Kléman, *J. Physique*, **31**, 1041 (1970).
36. J. Rault, *Mol. Cryst. Liq. Cryst.*, **16**, 143 (1972).
37. Y. Bouligand, *J. Physique*, **33**, 715 (1972).
38. Y. Bouligand, *J. Physique*, **35**, 959 (1974).
39. M. Kawachi, O. Kogure and K. Kato, US Patent 3936825.
40. Y. Bouligand, *J. Physique*, **34**, 1011 (1973).
41. M. Kléman, "Points.Linges.Parois.", Tome I, Edition de Physique, Paris (1978).
42. A. Saupe, *Mol. Cryst. Liq. Cryst.*, **21**, 211 (1973).
43. L. J. Yu and M.-M. Labes, *Mol. Cryst. Liq. Cryst.*, **28**, 423 (1974).
44. M. Luban, D. Mukamel and Sh. Shtrikman, *Phys. Rev.*, **A10**, 360 (1974).
45. M. Luban, Sh. Shtrikman and J. Isaacson, *Phys. Rev.*, **A15**, 1211 (1977).
46. T. B. Harvey, *Mol. Cryst. Liq. Cryst. Lett.*, **34**, 225 (1977).
47. A. I. Derzhanski, S. B. Naidenova and B. Taneva, *Compt. Rend. Acad. Bulg. Sci.*, **31**, 517 (1978).
48. F. P. Price and Sh. S. Bak, *Mol. Cryst. Liq. Cryst.*, **29**, 225 (1975).
49. T. Uchida, Ch. Shishido and M. Wada, *El. Comm. Jap.*, **57-C**, 103 (1974).
50. G. Chilaya, S. Aronishidze, K. Vinokur, S. Ivchenko and M. Brodzeli, *Acta Phys. Pol.*, **A54**, 655 (1978).
51. V. N. Tsvetkov, Ph. Dr. Thesis, Leningrad (1974).
52. H. P. Hinov, *Mol. Cryst. Liq. Cryst.*, **74**, 1789 (1981).
53. H. P. Hinov, L. K. Vistin' and Ju. G. Magakova, *Kristallogr.*, **23**, 583 (1978).
54. H. P. Hinov and L. K. Vistin', *J. Physique*, **40**, 269 (1979).
55. H. P. Hinov, *Z. Nat.*, **37a**, 334 (1982).
56. H. P. Hinov, *Mol. Cryst. Liq. Cryst.*, **89**, 227 (1982).
57. H. P. Hinov, Ph. Dr. Thesis, Sofia (1980).
58. H. P. Hinov and A. I. Derzhanski, *Liq. Cryst. Ord. Fl.*, **4**, in press (1983).
59. M. Nakamura, *J. Appl. Phys.*, **52**, 4561 (1981).
60. H. P. Hinov and D. Riviére, to be published.
61. H. P. Hinov and G. Klose, to be published.
62. B. R. Ratna and R. Shashidhar, *Mol. Cryst. Liq. Cryst.*, **42**, 113 (1977).
63. J. W. Park and M. M. Labes, *J. Appl. Phys.*, **48**, 22 (1977).
64. M. Nakamura and M. Ura, *J. Appl. Phys.*, **52**, 210 (1982).
65. J. Cognard, *Mol. Cryst. Liq. Cryst. Lett.*, **64**, 331 (1981).
66. Sh. Naemura, *J. Appl. Phys.*, **51**, 6149 (1980).
67. Sh. Naemura, *J. Phys. Colloq.*, **40**, C3-514 (1979).
68. J. Cheng and G. D. Boyd, *Appl. Phys. Lett.*, **6**, 444 (1979).
69. K. U. Denitz, T. K. Bhattacharaya and C. Manochar, *Proc. Nucl. Ph. and Solid State Phys. Symp.*, Calcutta (1975).
70. W. E. L. Haas and J. E. Adams, *Appl. Phys. Lett.*, **25**, 535 (1974).